



HAL
open science

Design of a 2-DoF Haptic Device for Motion Guidance

Lisheng Kuang, Maud Marchal, Marco Aggravi, Paolo Robuffo Giordano,
Claudio Pacchierotti

► **To cite this version:**

Lisheng Kuang, Maud Marchal, Marco Aggravi, Paolo Robuffo Giordano, Claudio Pacchierotti. Design of a 2-DoF Haptic Device for Motion Guidance. EuroHaptics 2022 - International conference on Haptics: Science, Technology, Applications, May 2022, Hamburg, Germany. pp.1-8. hal-03614070

HAL Id: hal-03614070

<https://inria.hal.science/hal-03614070v1>

Submitted on 19 Mar 2022

HAL is a multi-disciplinary open access archive for the deposit and dissemination of scientific research documents, whether they are published or not. The documents may come from teaching and research institutions in France or abroad, or from public or private research centers.

L'archive ouverte pluridisciplinaire **HAL**, est destinée au dépôt et à la diffusion de documents scientifiques de niveau recherche, publiés ou non, émanant des établissements d'enseignement et de recherche français ou étrangers, des laboratoires publics ou privés.



Distributed under a Creative Commons Attribution 4.0 International License

Design of a 2-DoF Haptic Device for Motion Guidance^{*}

Lisheng Kuang¹, Maud Marchal², Marco Aggravi¹,
Paolo Robuffo Giordano¹, and Claudio Pacchierotti¹

¹ Univ Rennes, CNRS, Inria, IRISA – France

² Univ Rennes, INSA Rennes, CNRS, Inria, IRISA – France and IUF – France
{name.surname}@irisa.fr

Abstract. We present a 2-degrees-of-freedom (2-DoF) haptic device, which can be either used as a grounded or a hand-held device. It is composed of two platforms moving with respect to each other, actuated by two servomotors housed in one of structures. The device implements a rigid coupling mechanism between the two platforms, based on a three-legged 3-4R constrained parallel linkage, with the two servomotors actuating two of these legs. The device can apply position/kinesthetic haptic feedback to the user hand(s). This paper presents the device and its kinematics, together with a human subjects experiment where we evaluate its capabilities to provide meaningful directional information.

Keywords: Motion guidance

1 Introduction

Kinesthetic haptic interfaces have been very popular in the past, for applications ranging from industrial to surgical robotics. Researchers have designed many different types of such interfaces, focusing on improving their, e.g., peak force, bandwidth, workspace, and/or price, according to the target field of application. In this respect, we can identify two main categories of kinesthetic interfaces: grounded and ungrounded. Grounded devices have their base placed on an external support, such as a table, while ungrounded devices have their base on the user’s body [8]. Grounded kinesthetic devices include popular commercial kinesthetic systems such as the Virtuoso (Haption, FR), Omega.x (Force Dimension, CH), Falcon (Novint Tech., USA) and the Phantom (Geomagic, 3D Systems, USA) series. More recently, in research, Jang et al. [3] presented a grounded isometric interaction device to induce whole-body interaction; Okui et al. [7] designed a delta-type 4-degrees-of-freedom (4-DoF) grounded haptic device actuated with a magnetorheological clutch, thus able to adjust its stiffness and viscosity; and Satler et al. [10] devised a portable interface composed of controlled wheel torques to render forces to a user handle placed on the top of the device. On the other hand, ungrounded kinesthetic devices come in very different forms, spanning from hand-held devices for gaming and VR interaction [5,12] or guidance [11,13] to body-worn exoskeletons [1,9].

^{*} This work has received funding from the Inria Défi project “DORNELL” and the China Scholarship Council No. 201908440309.

This paper presents a 2-degrees-of-freedom (2-DoF) kinesthetic device that can be either attached onto an external support or held between the two hands. Its design is inspired by the anti-parallelogram mechanism [6] featuring a quaternion joint [4]. It is composed of two structures, connected by three articulated legs which are in turn actuated by two servo motors. By moving with respect to each other, they can provide the user with directional information.

2 Device design and actuation

The proposed device is shown in Fig. 1. A video is available at <https://youtu.be/vc6B-00j590>.

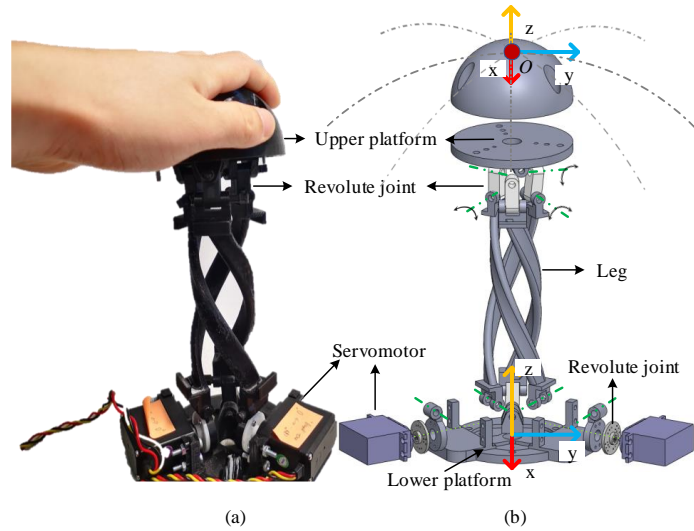


Fig. 1. The device is composed of two servo motors actuating an anti-parallelogram mechanism moving two platforms with respect to each other. (a) Device in its grounded configuration, with the lower platform secured to an external support and the user hand posed on the upper one. The device can be either used as a grounded interface, like in this figure and in our experiment of Sec. 3, or it can be held between the two hands (see the video for this configuration). (b) CAD of the device. The grey dotted lines show the surface of the sphere on which the upper platform moves. The spherical cap posed on the upper platform makes the interaction with the user hand more comfortable. Of course, it can be changed with other shapes according to the task at hand.

2.1 Mechanism and Structure

The design of the proposed device is inspired by the principle of the anti-parallelogram mechanism [6], which consists of three identical supporting linkages forming an interlaced structure with no interference between them [4]. Compared to standard serial mechanisms, parallel mechanisms enable fast dynamics and high payload with relatively small size and low weight. Moreover, a large range of motion and uniform manipulability can be obtained by choosing appropriate dimensional parameters and actuation.

As shown in Fig. 1, the device consists of two platforms, a lower and an upper platforms, connected by three legs each having a spiral curved link. The device has dimensions of $15 \times 15 \times 23$ cm and weighs 150 g. The two ends of each link are connected with two serial revolute joints to the platforms, forming a 3-4R coupling parallel mechanism which can move freely with 2 degrees of freedom, according to the orthogonal rolling motion on each leg [4]. If the lower platform is fixed on an external support (as in Fig. 1(a)), the motion of the upper platform is confined on the surface of a sphere centered in the center of the lower platform (see grey dotted lines in Fig. 1(b)). Two Hitech-625MG servo motors are attached to two legs on the lower platform. One revolute joint on the short linkage is mounted to the motor shaft, the other joint connects to the leg, as shown in Fig. 1. In this configuration, the two legs equipped with the servomotors have an active rotation on the lower joints and a passive rotation on the other three joints. By changing the actuation of the two motors, the upper platform can reach any point within its workspace (the surface of a sphere, as mentioned above). The graphical method using reciprocal screw system theory can be used [14] to analyze the mobility of the proposed parallel mechanism.

2.2 Kinematics Analysis

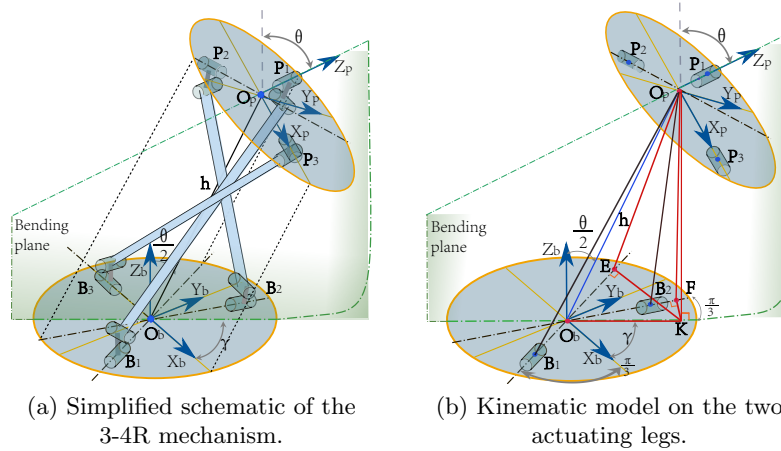


Fig. 2. Schematic of the proposed device.

We study the kinematics of the device so as to evaluate the relationship between the motion of the servomotors and that of the upper platform with respect to the lower one. As illustrated in Figs. 1 and 2, three legs are regarded as individual open-chain manipulators. The connection points between the upper platform and legs 1, 2, 3 are defined as P_1 , P_2 , P_3 , respectively, while the connection points between the lower platform and the legs is denoted by points B_1 , B_2 , B_3 . Let us consider the device in its grounded configuration, with the base attached to an external support. The coordinate frames of the upper (mobile)

and lower (static) platforms, $C_p(O_p - x_p y_p z_p)$ and $C_b(O_b - x_b y_b z_b)$, are fixed on their geometric centers, O_p and O_b , respectively. The frames are defined as indicated in Figs. 1 and 2.

The plane where the z_b and z_p axes coexist is defined as the bending plane, which is always perpendicular to the surfaces of the two platforms. Here, the orientation angle θ and bending angle γ denote the angle between z_b and z_p on the bending plane and the angle from the x_b axis to the bending plane, respectively. Considering the bending and orientation angles, the homogeneous transformation from C_b to C_p is as follows:

$$\begin{aligned} {}^b_p T &= R(Z, \gamma) R(Y, \frac{\theta}{2}) T(h) R(Y, \frac{\theta}{2}) R(Z, -\gamma) \\ &= \begin{bmatrix} 1 - 2C^2(\gamma)S^2(\frac{\theta}{2}) & -S(2\gamma)S^2(\frac{\theta}{2}) & C(\gamma)S(\theta) & hC(\gamma)S(\frac{\theta}{2}) \\ -S(2\gamma)S^2(\frac{\theta}{2}) & 1 - 2S^2(\gamma)S^2(\frac{\theta}{2}) & S(\gamma)S(\theta) & hS(\gamma)S(\frac{\theta}{2}) \\ -C(\gamma)S(\theta) & -S(\gamma)S(\theta) & C(\theta) & hC(\frac{\theta}{2}) \\ 0 & 0 & 0 & 1 \end{bmatrix} \end{aligned} \quad (1)$$

where $S(x) = \sin(x)$ and $C(x) = \cos(x)$, $R(., .)$ denotes a rotation, T an homogeneous transformation around the z axis, and h the distance between O_b and O_p , which is also the diameter of the sphere onto which the upper platform moves.

Geometrically, we can also derive the relationship (forward and inverse kinematics) between γ and θ with respect to the motor's inputs α_1 and α_2 . As shown in Fig. 2b, motor 1 is mounted at B_1 with the motor shaft rotating along B_1O_b , while motor 2 is mounted at B_2 , with its shaft rotating along B_2O_b . The motor's rotating angle is limited within $(-\pi/2, \pi/2)$. For any bending pose of the upper platform, O_p has a projection point K in the plane $B_1B_2B_3$. Obviously, O_pK is perpendicular to B_1O_b and B_2O_b , and it is in the bending plane. Moving perpendicularly from K to B_1O_b and B_2O_b , we obtain two pedal points, E , F , which lie in the shaft axis of motor 1 and motor 2, respectively. Right-angled triangle $\triangle O_pKE$ and $\triangle O_pKF$ share the same edge O_pK . As O_pE and O_pB_1 lie in the same plane $O_pO_bB_1$, then the rotation angle of motor 1, α_1 , is equal to $\angle O_pEK$, and that of motor 2, α_2 , is equal to $\angle O_pFK$. From a simple geometrical derivation, we obtain

$$\begin{aligned} \tan(\alpha_1) &= \tan(\angle O_pEK) = \frac{O_pK}{EK} = \frac{O_pK}{O_bK \sin(\gamma + \frac{\pi}{3})} \\ &= \frac{h \cos \frac{\theta}{2}}{h \sin \frac{\theta}{2} \sin(\gamma + \frac{\pi}{3})} = \frac{1}{\tan \frac{\theta}{2} \sin(\gamma + \frac{\pi}{3})} \end{aligned} \quad (2)$$

$$\tan(\alpha_2) = \tan(\angle O_pFK) = \frac{O_pK}{FK} = \frac{1}{\tan \frac{\theta}{2} \sin(\gamma - \frac{\pi}{3})} \quad (3)$$

3 Experimental evaluation

We carried out an experiment evaluating the capabilities of the device in providing directional/motion information. The device renders a set of shapes with its end-effector, i.e., the moving upper platform, that users are asked to recognize.

3.1 Setup

The experimental setup is shown in Fig. 1. The device is used in its grounded configuration, with the lower platform attached to a table. Users are seated in front of the device and are asked to place their dominant hand on the device upper platform. A cardboard prevents the user from seeing his or her hand on the device during the experiment. A computer screen is also placed in front of the user, from which he or she can receive information about the experiment and answer the related questions.

3.2 Participants

Fourteen subjects (1 female and 13 males, aged from 23 to 33 years) participated in the experiment. Six are left-handed, eight are right-handed. Participants received an information sheet with the experiment details and signed a consent form. The study has been approved by Inria’s ethics committee (Saisine 513).

3.3 Procedure

The experiment is divided in two blocks, carried out one after the other.

In the first one, the device moves along eight linear patterns, shown in Figs. 3a and 3c. We recall that the center of the upper platform O_p moves across the surface of a sphere having diameter h and centered at the center of the lower platform O_b (see Sec. 2.2). Each linear pattern starts from the resting position of O_p , then moves towards its designated direction and back, along a circular arc with chord of 20 cm (see also the video). For example, the linear pattern referred to as “South” in Fig. 3, starts from the resting position of O_p , then moves towards the S (South) direction (see Fig. 3a), then back to the resting position of O_p , then moves towards the N (North) direction, and finishes in the resting position of O_p . All linear patterns start and finish in the resting position of O_p . The user sits on the South side of the device.

In the second block, the device moves along three shape patterns, shown in Figs. 4a and 4b. Similarly as before, these shapes are actuated over the surface of the sphere that is the workspace of our device. As indicated in Fig. 4a, they all start from a point located at the North of the resting position of O_p (named P in the Figure). Before starting the experiment, the experimenter explained the procedure to the user and spent about two minutes adjusting the chair armrest. Subjects placed their palm on the upper platform of the device and lean on the chair armrest to keep the forearm at the same level of the upper platform, ensuring maximum comfort. After each pattern was rendered, users were asked to select which pattern, in their opinion, the device just rendered. This choice was made through a GUI on the computer screen in front of the user. The device actuating all the patterns is shown at <https://youtu.be/vc6B-00j590>.

Each pattern was provided five times, yielding $(8 \text{ linear patterns} + 3 \text{ shape patterns}) \times 5 = 55$ repetitions of this pattern recognition task.

Immediately after the experiment, participants were asked to fill in a questionnaire where we asked which pattern was the harder/easier to recognize and if they had any further comment about the rendering and the experiment.

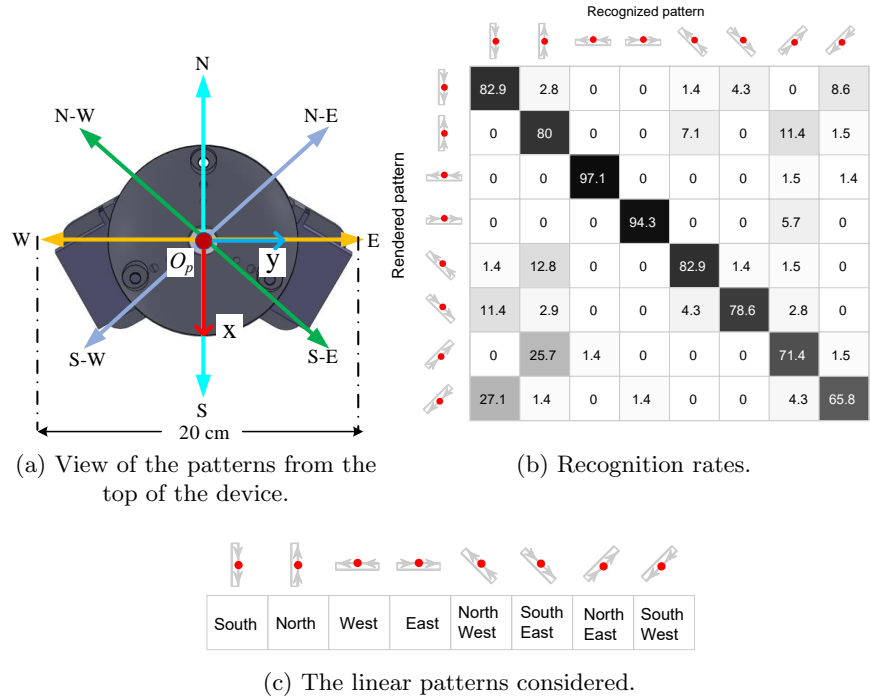


Fig. 3. Linear patterns. (a) The patterns as rendered by the device, view from the top of the upper platform; (b) recognition rates of linear patterns; (c) the linear patterns. All linear patterns start and finish in the resting position of O_p , moving along a circular arc having a chord of 20 cm.

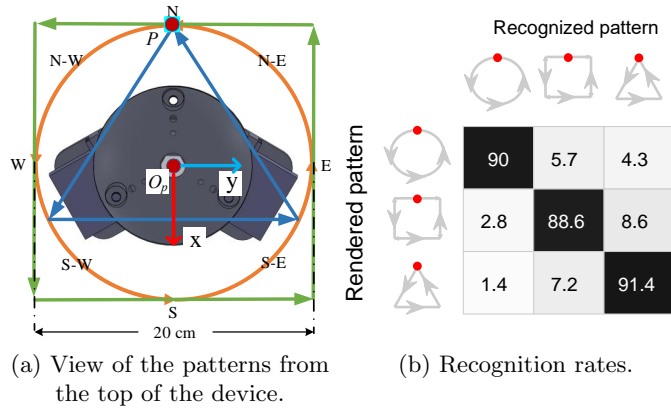


Fig. 4. Shape patterns. (a) The patterns as rendered by the device, view from the top of the upper platform. All shape patterns start and finish north of the resting position of O_p , in the point named P. (b) Recognition rates of shape patterns;

3.4 Results

Figs. 3b and 4b report the results of the experiment, in the form of two confusion matrices showing the percentage of recognition of the rendered vs. the recognized patterns. For the linear patterns the chance level is $1/8$ (12.5%), while for the shape patterns the chance level is $1/3$ (33.3%). The questionnaire showed that “East” and “West” linear patterns were considered as the easiest to identify, while the square shape pattern resulted to be the hardest. Diagonal linear patterns were reported to be harder to identify than other linear patterns.

4 Discussion and Conclusions

This paper presented a kinesthetic haptic device composed of two platforms connected by three interleaved legs. Two servo motors, actuating two of the three legs, can move the upper platform on the surface of a sphere centered in the lower platform. While the device can be used both in a grounded or hand-held configuration, this paper focused on the former. In this case, the lower base is firmly attached to an external support, and the upper platform moves so as to provide the user with haptic feedback.

We carried out an experimental evaluation of our device. 14 human subjects were asked to place their hand on the upper platform of the device and recognize the pattern being displayed. The device was commanded to render 8 linear and 3 shape patterns, which can be used to provide, e.g., navigational information. Results show a very high recognition rate for all patterns, with the highest and lowest recognition rate being 97.1% and 65.8%, respectively, with a chance level of 12.5%. For the linear patterns recognition, it was easier to recognize horizontal patterns (lateral-median motions with respect to the user, e.g., West and East patterns), while diagonal patterns were the hardest to recognize. The sense of motion along a certain pattern did not seem to affect much performance. The most common mistake was to identify diagonal patterns as anterior-posterior ones (North and South patterns). For the shape patterns recognition, recognition rates are very high in all conditions. In this case, subjects reported to be mostly relying on the number of edges being rendered by the device.

The design of this device shows also some limitations. First, in the current configuration, as we are using servo motors, the device is not backdrivable and cannot be used as a standard impedance-type haptic interface. Second, the motors are both placed on the same platform, which is a good idea if the device is used in a grounded configuration, but not ideal if held between the two hands. In a hand-held configuration, it is better to distribute the weight equally between the two platform, which should be straightforward to do.

Given such promising results, in the next future we plan to test a wider range of patterns, evaluating, e.g., the smallest change in orientation between two linear patterns and the smallest change in the number of edges between two shape patterns users can discriminate. We will also test the device when held between two hands, as well as the performance of the device in terms of resolution, precision, repeatability, and maximum output force. This device was developed within a larger effort to design a multi-modal haptic handle for various

mobility aids, e.g., power wheelchairs, walkers, prewalkers. For this reason, we also plan to test this device effectiveness in rendering directional information when mounted on one of these mobility aids, similarly to [2].

References

1. Chinello, F., Malvezzi, M., Prattichizzo, D., Pacchierotti, C.: A modular wearable finger interface for cutaneous and kinesthetic interaction: control and evaluation. *IEEE Trans. Industrial Electronics* **67**(1), 706–716 (2019)
2. Devigne, L., Aggravi, M., Bivaud, M., Balix, N., Teodorescu, C.S., Carlson, T., Spreters, T., Pacchierotti, C., Babel, M.: Power wheelchair navigation assistance using wearable vibrotactile haptics. *IEEE Trans. Haptics* **13**(1), 52–58 (2020)
3. Jang, B.g., Kim, G.J.: Evaluation of grounded isometric interface for whole-body navigation in virtual environments. *Computer Animation and Virtual Worlds* **25**(5–6), 561–575 (2014)
4. Kim, Y.J., Kim, J.I., Jang, W.: Quaternion joint: Dexterous 3-dof joint representing quaternion motion for high-speed safe interaction. In: *IEEE/RSJ International Conference on Intelligent Robots and Systems (IROS)*. pp. 935–942 (2018)
5. Kovacs, R., Ofek, E., Gonzalez Franco, M., Siu, A.F., Marwecki, S., Holz, C., Sinclair, M.: Haptic pivot: On-demand handhelds in vr. In: *Proc. Annual ACM Symposium on User Interface Software and Technology*. pp. 1046–1059 (2020)
6. Okada, M., Nakamura, Y.: Development of a cybernetic shoulder—a 3-dof mechanism that imitates biological shoulder motion. *IEEE Trans. Robotics* **21**(3), 438–444 (2005)
7. Okui, M., Kobayashi, M., Yamada, Y., Nakamura, T.: Delta-type four-dof force-feedback device composed of pneumatic artificial muscles and magnetorheological clutch and its application to lid opening. *Smart Materials and Structures* **28**(6), 064003 (2019)
8. Pacchierotti, C., Sinclair, S., Solazzi, M., Frisoli, A., Hayward, V., Prattichizzo, D.: Wearable haptic systems for the fingertip and the hand: taxonomy, review, and perspectives. *IEEE Trans. Haptics* **10**(4), 580–600 (2017)
9. Sarac, M., Solazzi, M., Frisoli, A.: Design requirements of generic hand exoskeletons and survey of hand exoskeletons for rehabilitation, assistive, or haptic use. *IEEE Trans. haptics* **12**(4), 400–413 (2019)
10. Satler, M., Avizzano, C.A., Ruffaldi, E.: Control of a desktop mobile haptic interface. In: *IEEE World Haptics Conference (WHC)*. pp. 415–420 (2011)
11. Spiers, A.J., Dollar, A.M.: Design and evaluation of shape-changing haptic interfaces for pedestrian navigation assistance. *IEEE Trans. Haptics* **10**(1), 17–28 (2016)
12. de Tinguy, X., Howard, T., Pacchierotti, C., Marchal, M., Lécuyer, A.: Weatavix: wearable actuated tangibles for virtual reality experiences. In: *International Conference on Human Haptic Sensing and Touch Enabled Computer Applications*. pp. 262–270 (2020)
13. Walker, J.M., Zemiti, N., Poignet, P., Okamura, A.M.: Holdable haptic device for 4-dof motion guidance. In: *IEEE World Haptics Conference (WHC)*. pp. 109–114 (2019)
14. Yu, J., Dong, X., Pei, X., Kong, X.: Mobility and singularity analysis of a class of two degrees of freedom rotational parallel mechanisms using a visual graphic approach. *Journal of Mechanisms and Robotics* **4**(4) (2012)